IET Radar Sonar and Navigation, Volume 13, Issue 10, 2019, pp. 1705-1712
https://ieeexplore.ieee.org/document/8870308

A novel outlier removal method for two-dimensional radar odometry

ISSN 1751-8644
doi: 0000000000
www.ietdl.org

Antonio F. Scannapieco

[1] *Centre for Electronic Warfare, Information, and Cyber, Cranfield University, Defence Academy of the United Kingdom, Shrivenham, SN6 8LA UK*
** E-mail: a.scannapieco@cranfield.ac.uk*

Abstract: Autonomous navigation of platforms in complex environments has a key role in many applications. However, the environmental conditions could negatively affect the performance of electro-optical sensors. Hence, the idea of using radar odometry has been recently developed. However, it suffers from the presence of outliers in the scene as its electro-optical counterparts. This work presents a method to classify radar echoes as inliers or outliers for two-dimensional radar odometry, based on their range rate and bearing angle. The range rate and bearing angle are in fact combined to give a classification value, different for each target. At each acquisition time, the median of all classification values is computed. Since classification values of stationary targets, i.e. the inliers, cluster around the median, while moving targets, i.e. the outliers, exhibit larger distance from the median, stationary targets and moving targets can be separated. This is also useful for Sense-and-Avoid purposes. The method has been tested in simulated scenario to show effectiveness in detecting outliers and in real case scenario to demonstrate significant improvement in reconstruction of trajectory of platform, keeping the final error around 10% of the travelled distance. Further improvement is envisaged by integrating the method in the target tracking strategy.

1 Introduction

Autonomous operations by robots and Unmanned Aircraft Systems (UAS) have been addressed in several works and for several applications in the last years. The fast development of new technologies and hardware miniaturization led the interest of the scientific community towards applications to be carried in complex scenarios with small platforms, both terrestrial and aerial, with different levels of autonomy. Given the very nature of envisaged scenarios, the Global Navigation Satellite System (GNSS) reference signal is often neither available nor reliable, causing the navigation aspect of autonomy to be tackled with different sensors. Inertial Measurement Units (IMUs) cannot be the only source of self-positioning information, owing to fast-growing errors. Additionally, they do not provide information about the surrounding scene, which is equally important in unknown environments. Typical electro-optical sensors used on board small robots or small UAS, such as cameras or LIDARs, are very sensitive to illumination and environmental conditions. Performance of radar sensors, on the contrary, is less dependent on the environment. For this reason, several techniques have been studied for navigation of platform in GNSS-denied environment. One field particularly investigated is the indoor navigation. Many studies rely on the deployment in indoor environment of active radiofrequency (RF) stations to be detected with Ultra Wide Bandwidth (UWB) radars. Tiemann et al. [1] use UWB receivers to allow cooperative UAV navigation indoors. Zwirello et al. [2] show an indoor inertial positioning system aided by UWB receiver, with a set of RF active access points in the scene. Hybrid inertial and UWB indoor navigation is also presented by Kagawa et al. [3], He et al. [4], and Li et al. [5]. Tiemann et al. [6] perform indoor UWB Simultaneous Localization and Mapping (SLAM) with known anchor tags. Other UWB navigation solutions with known position of transmitters are presented in Tiemann et al. [7], Kaniewski et al. [8] and Krishnan et al. [9]. It is also worth noting that in Kumar et al. [10] a bistatic Frequency Modulated Continuous Wave (FMCW) radar is used to localize the active tags indoors. All these methods rely on knowledge of position of transmitters. Hence, they are not applicable to all the cases when the environment is unknown. A solution to address unknown environment is presented by Marck et al. [11], proposing a rotating small 24 GHz FMCW radar to achieve indoor SLAM. The rotating radar is manufactured by TNO. In the paper, the navigation solution is provided with Iterative Closest Point (ICP) solution, which is however sensible to outliers. Vivet et al. [12] also propose a rotating FMCW radar to address the SLAM problem, not indoors but in GNSS-challenging environment. The radar weighs 10 kg and might be not used for small robots. However, the work also addresses the Doppler effect and tackles the problem of outliers in radar measurements by using Random Sample Consensus (RANSAC) to establish coherence in the measurements and discard moving targets. Kauffman et al. [13] show a UWB Orthogonal Frequency Division Multiplexed (OFDM) system for navigation in unknown terrain. The assumptions made are that targets are randomly positioned and the radar is in side-looking observation to achieve SAR imaging. The method is tested against simulated data. Deissler et al. [14] propose indoor SLAM to reconstruct shape of the environment in which a robot is moving. The SLAM is based on a bistatic UWB radar, bio-inspired by bats, and it also fuses odometry information coming from the wheels of the robot. Cole et al. [15] use an UWB-OFDM radar to detect indoor doorways and perform navigation through the doorways. Baucher et al. [16] illustrate an UWB-based dead-reckoning system for a indoor terrestrial robot that exploit signal from targets of fortune. Very few strong targets are however present in the scene. The concept of radar odometry (RO) for autonomous navigation has been also introduced in literature recently. Kauffman et al. [17] use UWB-OFDM fused through Extended Kalman Filter (EKF) to obtain aircraft position. Approaches to RO proposed in Quist et al. [18, 19] are tailored to fixed-wing UAS. The data are acquired with high performance Synthetic Aperture Radar (SAR) flying on a Cessna aircraft. In [19] RANSAC is used to discard outliers. An approach towards small- and micro-UAS in a GNSS-challenging scenario is presented by Scannapieco et al. [20, 21]. Both works address RO with commercial ultralight FMCW radar in environments that can be significantly cluttered, hindering reliable extraction of many strong and stable scatterers. Furthermore in [21] differences in radar outputs from different scenes are shown. RO in [20, 21] are affected by outliers. Finally, Mostafa et al. [22] propose a method in which the platform velocity computed by radar is used to assist the visual odometry (VO). However, the radar-only trajectory is not computed.

In all the different previous works, it has been shown the importance of removing outliers to achieve proper self-localization of the

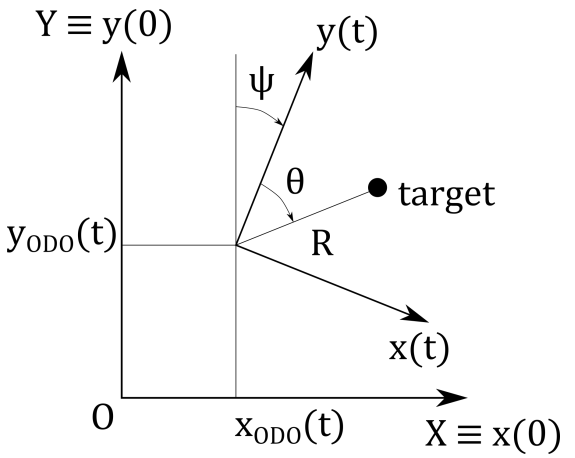

Fig. 1: Absolute reference frame and radar reference frame.

platform. The methods presented in [18, 19] use high-performance SAR, but RO with lightweight commercial radars can be easily addressed with small UAS and robots. Hence, methods to remove outliers for that RO approach should be found.

This paper aims at introducing a new method to detect outliers in the radar tracks for two-dimensional radar odometry in multi-target, GNSS-denied/challenging, unknown, and complex environments, thus enhancing the quality of dead-reckoning navigation solution. Furthermore, the new method is also able to provide additional information such as the classification of targets as stationary and moving targets, their position, and an estimate of platform velocity. Section 2 presents the assumptions made and the theoretical steps to achieve the novel outlier removal method, then Section 3 illustrates results achieved with the method in both simulated and real environment.

2 Modeling and Method

The system modelled in the present research is a radar operating in two dimensions. This assumption is motivated by the fact that for many applications with ground robots two principal dimensions are of main interest for navigation. Moreover, lightweight off-the-shelf radars [23–25] that can be relevant to RO on small platforms have large field of view (FOV) in azimuth and smaller FOV in elevation. This makes more reasonable a two-dimensional approximation, since targets observed are not too distant from the radar azimuth plane.

The model of radar used in this work is able to obtain range and bearing of each target. In general, range and bearing angle of targets can be obtained with different techniques. For example, multilateration with a radar network in multiple target environment is shown by Folster et al. [26] and by Szullo et al. [27]. Scanning radar is presented by Sugimoto et al. [28]. Phase interferometry is also feasible if two or more antennas are available, as explained in [20].

The other main approximation is that the radar is forward-looking. This means that the boresight direction of the radar is aligned with direction of motion of the platform. Different solutions, like scanning radars or SARs, can be used to retrieve map, but are out of the scope of this paper.

Under these assumptions and given a radar reference frame centred in the radar receiver with y direction oriented towards the direction of motion and x oriented perpendicular to y (see Fig. 1), the equations for range and bearing of every i-th target are

$$R_i\left(t\right) = \sqrt{x_i\left(t\right)^2 + y_i\left(t\right)^2} \tag{1}$$

$$\theta_i\left(t\right) = \tan^{-1}\left(\frac{x_i\left(t\right)}{y_i\left(t\right)}\right) \tag{2}$$

Range and bearing information for each target in the scene can be efficiently extracted from radar signal after some processing and

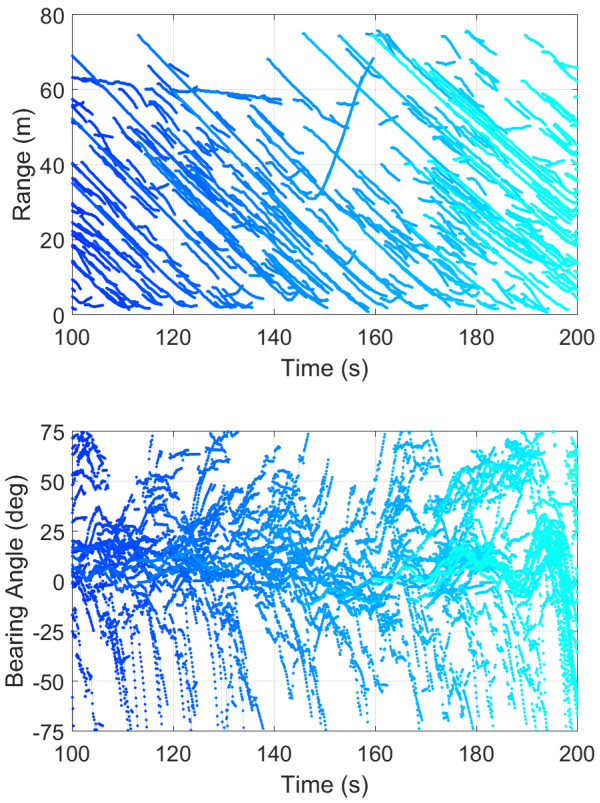

Fig. 2: Example of tracked targets in real scene. Each color corresponds to a track.

Constant False Alarm Rate (CFAR) adaptive thresholding [20]. Then the multiple-target tracking (MTT) associates every range-bearing couple to target tracks. Since a Kalman Filter (KF) is used in the MTT, the tracks are less noisy than the measurements.

An example of output of radar MTT for a platform moving in complex environment is shown in Fig. 2. MTT tracks all detected targets, which is desirable to have a complete awareness of the surrounding environment. However, as it can be seen in the magnification in Fig. 3, also strong moving targets can be tracked. This might represent a problem when retrieving the platform own-motion by means of odometry, since odometry makes use of stationary targets.

The main objective is therefore to separate stationary targets from moving targets within the set of tracks. Fig. 2 shows that stationary strong targets exhibit a similar behaviour in range. That is, stationary targets have similar slope due to the platform moving towards or away from them. This suggests that it can be possible to use the range rate of each target to separate moving targets and stationary targets. The range rate is obtained as the time first derivative of Eq. (1), as

$$\dot{R}_i = \frac{x_i\dot{x}_i + y_i\dot{y}_i}{\sqrt{x_i\left(t\right)^2 + y_i\left(t\right)^2}} \tag{3}$$

where $\dot{x}_i$ and $\dot{y}_i$ are the time derivatives of x and y in the radar reference frame.

Since the y_i coordinate of each target in the modelled radar reference frame is always positive, it is possible to manipulate Eq. (3) into

$$\dot{R}_i = \frac{\dot{y}_i + \tan\theta_i\dot{x}_i}{\sqrt{1 + \tan^2\theta_i}} \tag{4}$$

Eq. (4) shows that the range rate of a single target depends non-linearly on the bearing angle. As such, range rate in the form of Eq. (4) cannot be used as a parameter to estimate whether a target

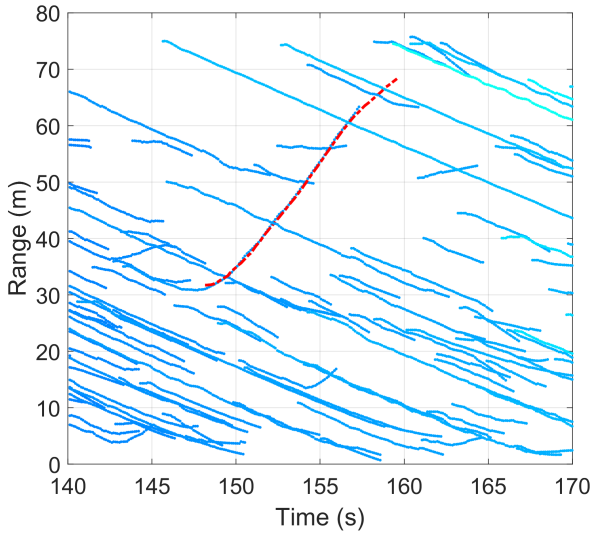

Fig. 3: Example of tracked targets in real scene. Magnification. The dashed red track represents a target moving away from the platform.

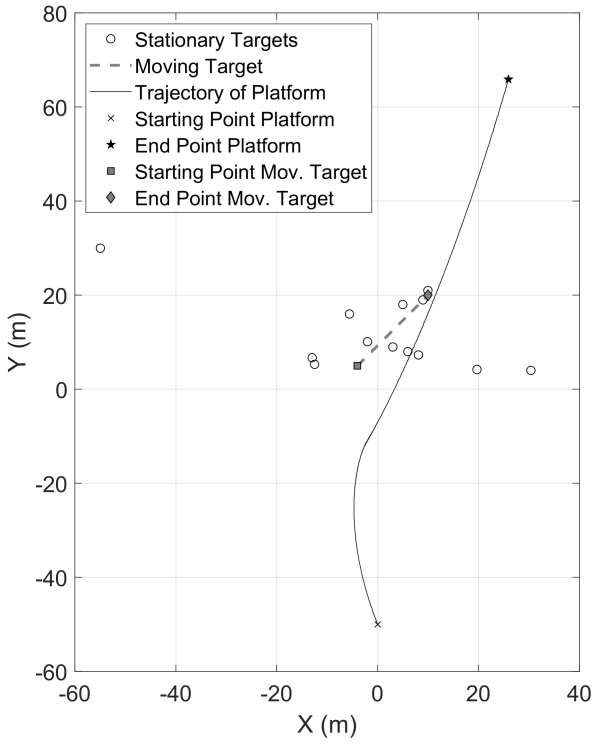

Fig. 4: Simulated scene with stationary targets and one moving target.

is stationary or moving. In order to provide insightful explanation to this problem, a scene with platform housing a radar, stationary targets, and one moving target has been simulated (see Fig. 4). The range and bearing angle output for each target is shown in Fig. 5 and the range rate computed according to Eq. (4) is presented in Fig. 6. It is evident that it is not possible to discriminate clearly the stationary targets from the moving one.

However, recalling that:

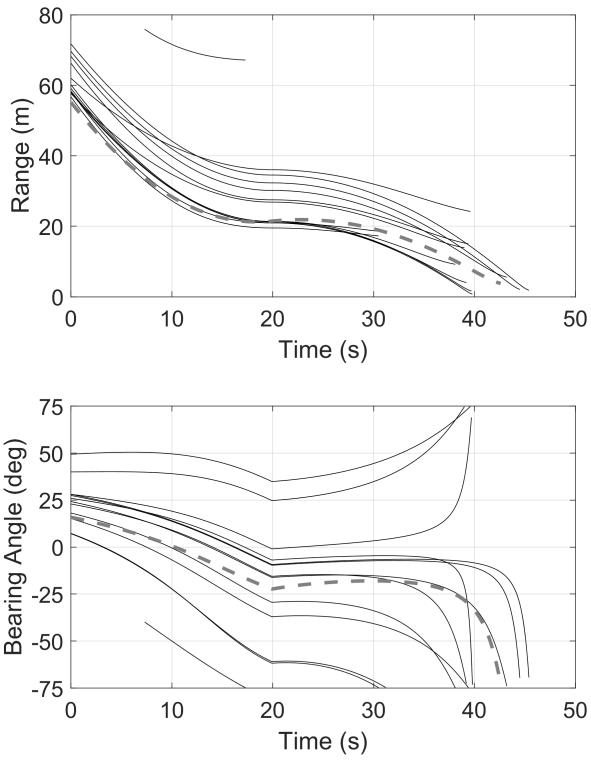

Fig. 5: Simulated scene with stationary targets and one moving target. Range and Bearing angle of stationary (black) and moving (dashed gray) targets.

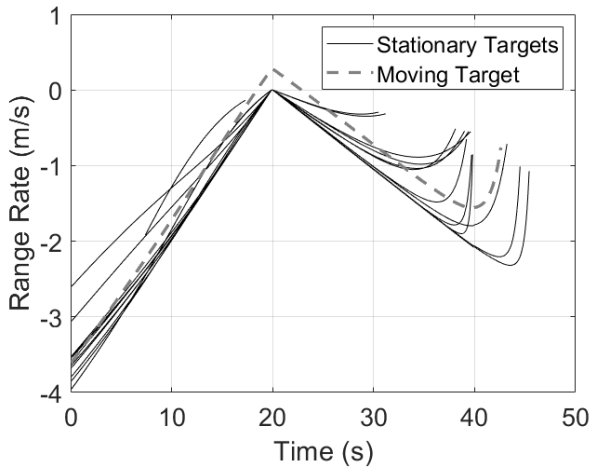

Fig. 6: Simulated scene with stationary targets and one moving target. Range Rate of stationary and moving targets. The bearing angle affects the result and there is no clear separation between targets.

1. the motion is supposed to be mainly along the forward-direction without any significant lateral slip, i.e. that for static targets

$$y_i > x_i \tag{5}$$

2. the 3-dB FOV of the radar is limited, that is, the tangent of the bearing angle affects very little the overall value

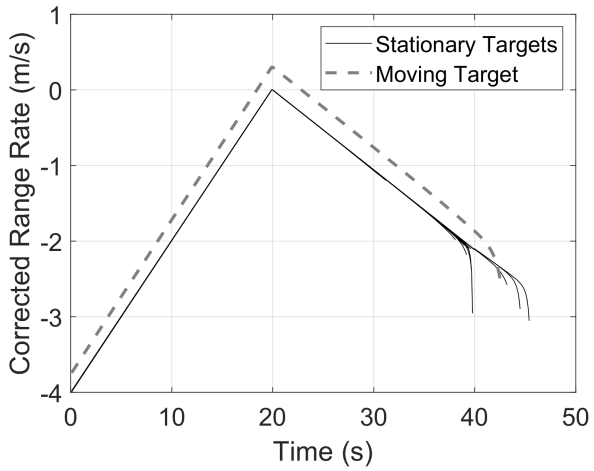

Fig. 7: Simulated scene with stationary targets and one moving target. Corrected Range Rate for outlier detection.

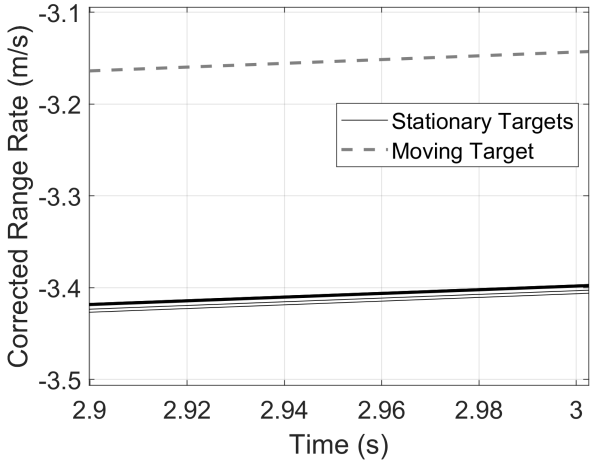

Fig. 8: Simulated scene with stationary targets and one moving target. Corrected Range Rate for outlier detection. Magnification.

then the parameter that can be used to separate moving targets from stationary targets is

$$T_{\mathrm{w},i} = \dot{R}_i \sqrt{1 + \tan^2 \theta_i} = \dot{y}_i + \tan\theta_i \dot{x}_i \tag{6}$$

Under these assumptions, stationary targets will exhibit very close values of $T_{\mathrm{w},i}$, even though not exactly equal, while moving targets will in general differ. The general trend of the corrected range rate for the same simulated scene is shown in Fig. 7. It is clearly possible to separate the moving target from stationary targets during most of the trajectory. It has to be noted that the separation fails when the targets are at extreme bearing angles. However, in general the echoes at such bearing angles might be fainter than the ones in the radar main lobe, thus being discarded. Fig. 8 shows in detail the behaviour of corrected range rate for stationary targets. Even though they do not have the same value, they are very close, compared to the moving target.

This observation suggests that a method to make use of the corrected range rate given by Eq. (6) to remove outliers could rely on the definition of Median Absolute Deviation (MAD) [29, 30]. Namely, for the case under analysis,

$$MAD = \underset{i}{\mathrm{median}} \left(\left| T_{\mathrm{w},i} - \underset{i}{\mathrm{median}} \left(T_{\mathrm{w},i} \right) \right| \right) \tag{7}$$

It is worth recalling that MAD is a robust estimator for variability of a function. Indeed, the relationship between the MAD and the estimated standard deviation of a population of values is given by statistics [30] as

$$\hat{\sigma} = k \cdot MAD \tag{8}$$

The value k depends on the statistical distribution of the points. In the case under analysis, it then depends on the statistical distribution of the corrected range rate. The additional assumption is that all the targets that lie within the 3-σ interval around the median value are considered inliers and, hence, stationary targets.

2.1 Remarking notes

It is worth noting that the approach presented in this work uses a definition of outliers concerning the radar odometry. Indeed, objects that are deemed outliers for the radar odometry passed through the CFAR as inliers. However, this kind of outliers can be used for Sense-and-Avoid (SAA) purposes. That is, once a target has been classified as moving (outlier), its position in a global reference frame XOY (see Fig. 1) can be derived as

$$X_i(t) = x_{\mathrm{odo}}(t) + R_i(t) \sin\left(\theta_i(t) + \psi(t)\right) \tag{9}$$

$$Y_i(t) = y_{\mathrm{odo}}(t) + R_i(t) \cos\left(\theta_i(t) + \psi(t)\right) \tag{10}$$

leading to enhanced awareness and enabling avoiding strategies.

Additionally, it has to be noted that the measurements of range and bearing angle are affected by noise. Since the method relies on values estimated with these measurements, the noise can be particularly detrimental to a successful identification. For this reason, the outliers are identified after the MTT track association, since the KF in the MTT block reduces the noise effects.

It has to be also highlighted that the corrected range rate of Eq. (6), under the assumptions of motion mainly along boresight direction and bearing angles not very big, can be approximated with the relative velocity $\dot{y}$. Hence, the modulus of median value of all the corrected range rates would give information on the modulus of velocity of the platform. It is clear that this is an approximated value, but could be used to help other sensors to refine estimates in sensor fusion strategies even if not related to radar odometry.

Finally, a more tight integration of the method in the MTT procedure could benefit for sure in a correct and successful identification of static targets, moving targets or just spurious radar echoes.

3 Tests and Results

The novel method has been tested against both simulated and real scenarios in order to assess possible drawbacks and actual performance.

3.1 Simulation

A simulated environment has been generated to assess the capability to discriminate moving targets from stationary targets with the proposed method. The simulation addresses noise-free measurements, which assumption can be considered valid enough in real cases when using measurements smoothed from the KF after the MTT. Furthermore, in this simulation the trajectories of both platform and moving targets are deterministic while the position of each stationary targets has been randomly generated. In particular, two moving targets and one hundred stationary targets have been used. The simulated radar specifics are listed in Table 1. The trajectory of the platform depends on the velocity modulus, v, and on the heading angle, ψ, defined as follows:

$$v = \begin{cases} 2\mathrm{m/s} - t\frac{1,5\mathrm{m/s}}{20\mathrm{s}} & 0\mathrm{s} < t < 20\mathrm{s} \\ 0,5\mathrm{m/s} - (t - 20\mathrm{s})\,\frac{0,05\mathrm{m/s}}{20\mathrm{s}} & 20\mathrm{s} < t < 40\mathrm{s} \\ 0,45\mathrm{m/s} + (t - 40\mathrm{s})\,\frac{0,95\mathrm{m/s}}{20\mathrm{s}} & 40\mathrm{s} < t \end{cases} \tag{11}$$

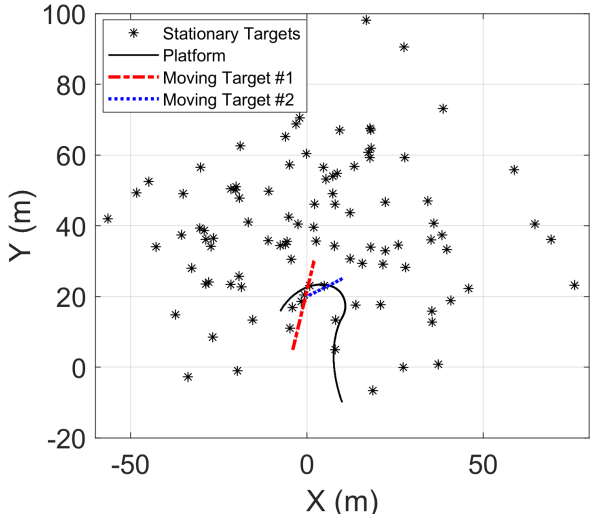

Fig. 9: Simulated scene with platform, stationary and moving targets.

$$\psi = \begin{cases} -20^\circ + t\frac{50^\circ}{20\text{s}} & 0\text{s} < t < 20\text{s} \\ 30^\circ - (t - 20\text{s})\,\frac{180^\circ}{40\text{s}} & 20\text{s} < t \end{cases} \tag{12}$$

The trajectory of the platform, the trajectories of moving targets and the position of stationary targets are represented in Fig.9. The range and bearing angle signatures of all the targets in the FOV of the radar are presented in Fig. 10. It can be seen that one moving target is not always present in the FOV of the radar.

The relative range rate signatures are shown in Fig. 11. It is clear that it is possible to separate stationary targets and moving targets. However, in some points the curves of moving targets cross the curves of stationary targets. This is shown in detail with magnification in Fig. 12, where the corrected range rate of first moving target intersects the corrected range rate curves of stationary targets. This can yield misleading information for few instants, but a proper design of MTT tracker and integration of the method in it can avoid errors. In order to highlight this possible issue, Fig. 13 shows the detected inliers and the number of false inliers, i.e. the moving targets classified as stationary. It can be seen that false inliers only appear when the values of corrected range rate crosses the values of stationary targets.

Finally, Fig.14 shows that the platform velocity estimated from the median value of corrected range rate values matches at very good degree of accuracy the ground truth provided by Eqs. (11)-(12).

3.2 Real environment

The method has been also applied to radar odometry with real data acquired during a campaign in a complex environment. The radar sensor, whose specifics are listed in Table 2, is the FMCW radar 24-GHz SENTIRE Radar by IMST [23]. The ground truth is provided by GPS receiver connected to a Pixhawk controller.

The environment is an urban canyon with moving targets, e.g. walking people, and a large number of man-made targets with different radar reflectivity. The difficulty associated with the presented real case is due to the fact that if two or more targets are at the same range, then the bearing angle will be combination of the bearing

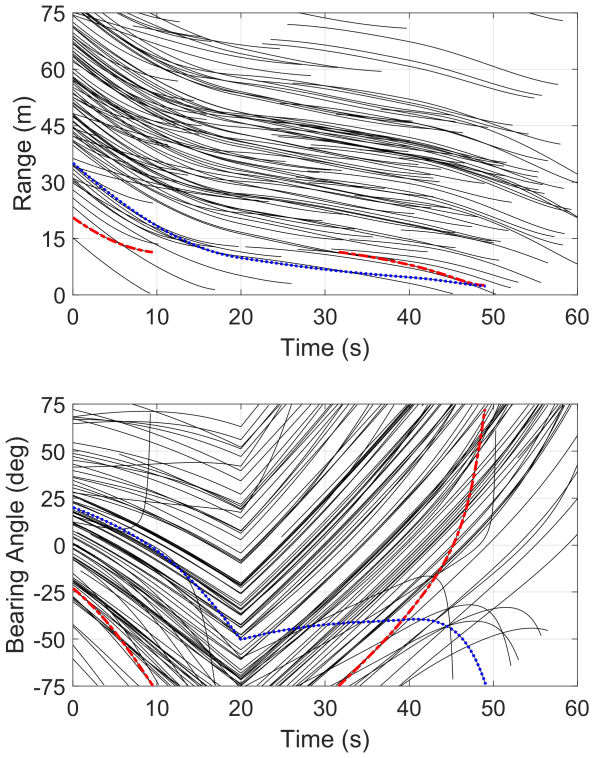

Fig. 10: Range (top) and bearing angle (bottom) for targets in simulated scene. Dash-dotted red lines are owing to first moving target, dotted blue lines are owing to the second moving target.

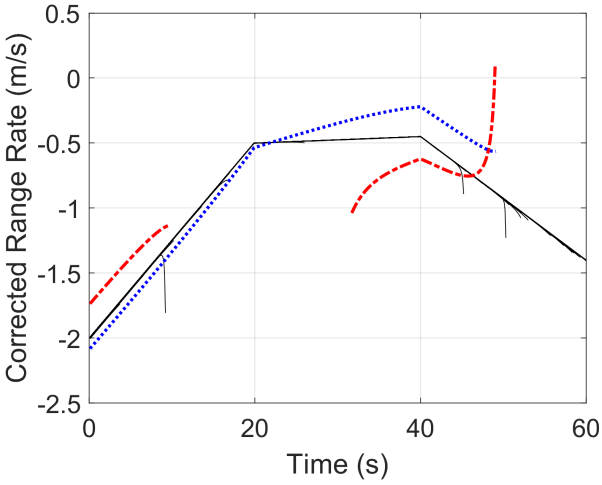

Fig. 11: Corrected range rate for targets in simulated tests. Dash-dotted red line is owing to first moving target, dotted blue line is owing to the second moving target.

Table 1 Simulated Radar Specifics

Maximum Range (m)	FOV Azimuth (°)
75	±75

Table 2 Real Radar Specifics

Range Resolution (cm)	FOV Azimuth (°)	Range Accuracy (cm)	Bearing Accuracy (°)
15	±60	< 10	≈ 5

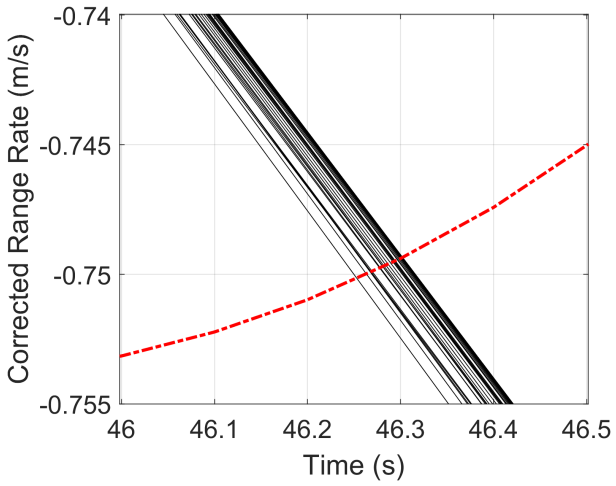

Fig. 12: Magnification of intersection between corrected range rate of moving target (dash-dot red) and corrected range rate of stationary targets (black).

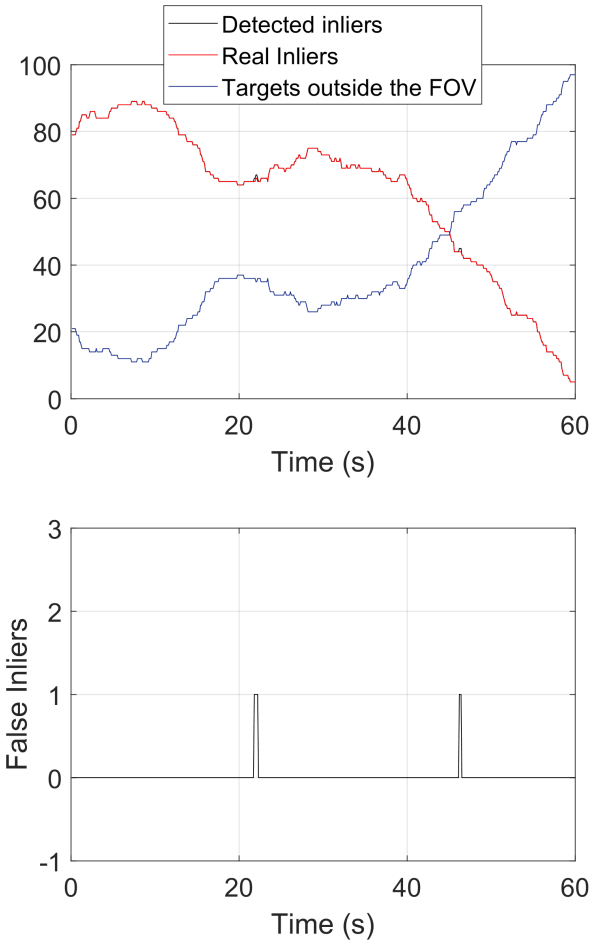

Fig. 13: Detected inliers and targets out the FOV and false inliers during the simulation.

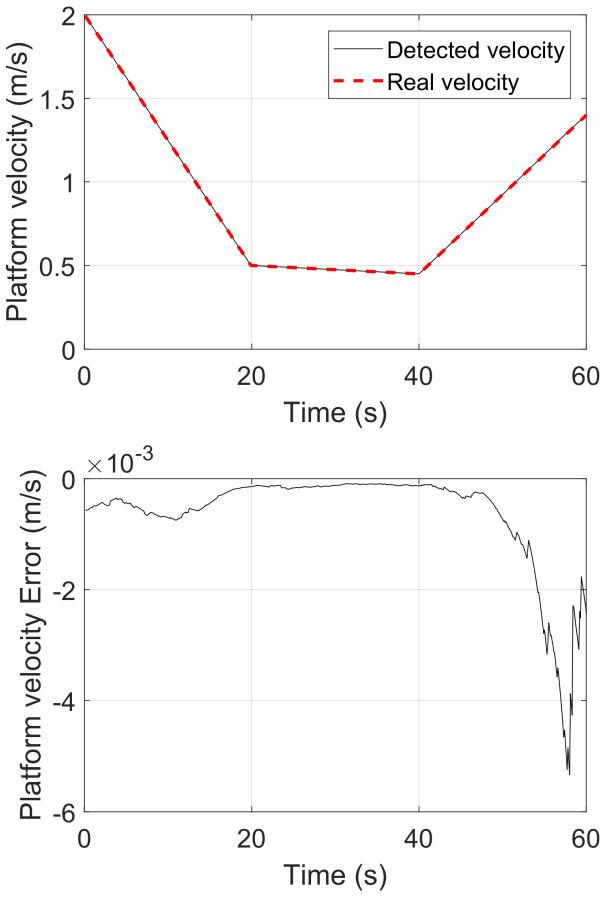

Fig. 14: Comparison between real and estimated platform velocity and error in platform velocity estimate.

angles of each target, as also described in [20, 21]. This, however, happens only for few instants, since the range for co-located targets will vary when platform moves.

A comparison of results from radar odometry solution with and without proposed outlier rejection method is shown in Fig. 15. The reconstructed trajectory is closer to ground truth when the proposed outlier rejection method is used. A full turn is recognized, even though in some points the heading reconstruction is not precise. The shape is mostly preserved, except for two points where the heading is not properly reconstructed. On the contrary, when keeping outliers, the angular reconstruction shows worse performance.

A more insightful analysis of performance can be obtained by looking at the errors of the RO-reconstructed trajectory with respect to the ground truth provided by GPS. Figg. 16-17 show that the error is kept below $20\mathrm{m}$ for the entire duration of the campaign. This is also confirmed by the absolute error shown in Fig. 18, where the error remains relatively steady after the first wrong heading association at around $t = 30\mathrm{s}$. It is interesting to show also the absolute error as percentage of the travelled distance (see Fig.19). After a certain distance, the error reaches a plateau. This means that it grows linearly with the travelled distance, which is a notable improvement with respect to the case with no outlier removal. Clearly, longer trajectories can provide further details about the performance of the solution.

It is worth highlighting, however, that the results seem to suggest that the radar odometry could also recover from errors. This is not strictly true, since the odometric solution is the sum of successive estimates and therefore the errors sum up. Nevertheless, it is possible that, owing to the fluctuations of target peaks within range cells, the

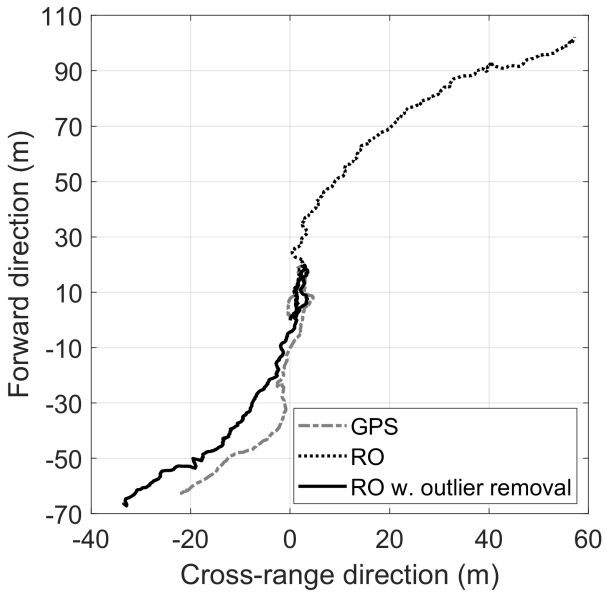

Fig. 15: Example of Radar Odometry with and without outlier removal correction in complex environment.

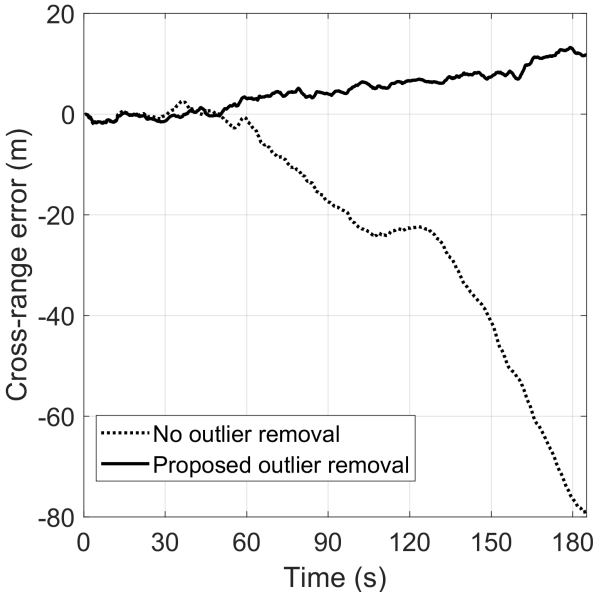

Fig. 17: Example of Radar Odometry with and without outlier removal correction in complex environment. Errors along cross-range direction.

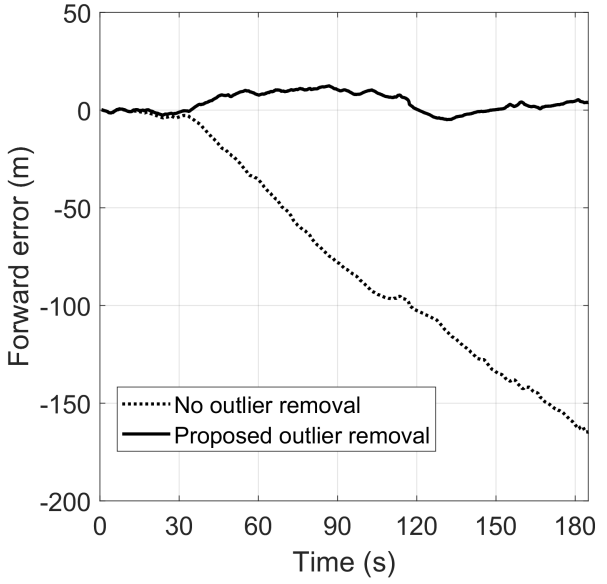

Fig. 16: Example of Radar Odometry with and without outlier removal correction in complex environment. Errors along forward direction.

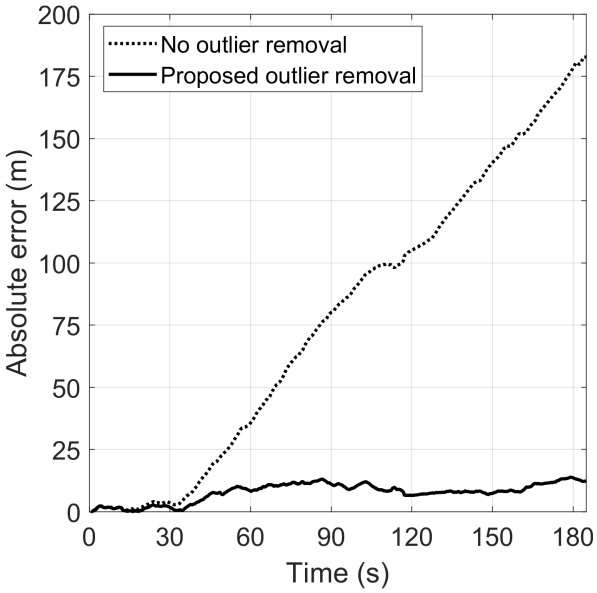

Fig. 18: Example of Radar Odometry with and without outlier removal correction in complex environment. Absolute errors.

errors had opposite sign in two successive steps and therefore mitigated the overall error. Further studies can address more carefully the highlighted point, but the proposed method of outlier rejection for radar odometry provides a great improvement to the final result.

Finally, platform velocity has been computed. The result, shown in Fig. 20, indicates that the estimate is close to ground truth but not as much as it does in simulations. However, it has to be noted that the radar-based estimate of platform velocity has smaller standard deviation around its average than velocity obtained by GPS has, the latter due to possible not good GPS signal condition. It is also interesting to note that when the full turn happens, a peak in platform velocity appears. This can be due to different targets appearing and disappearing very quickly in the FOV.

4 Conclusion

This paper presented a novel method to reject outliers when addressing the problem of platform navigation by means of two-dimensional Radar Odometry. The outliers for the RO are both moving targets and erroneous measurements survived to the filtering in the MTT. The method is based on the definition of corrected range rate and makes use of robust estimator. A significant improvement in the two-dimensional radar odometry is shown. Furthermore, the classification of targets, as stationary or moving ones, enables positioning of moving and stationary radar targets in a global map, which can be useful for Sense-and-Avoid purposes, and allows a preliminary estimate of platform velocity modulus. Further integration of the outlier rejection strategy into the MTT can possibly provide more benefits

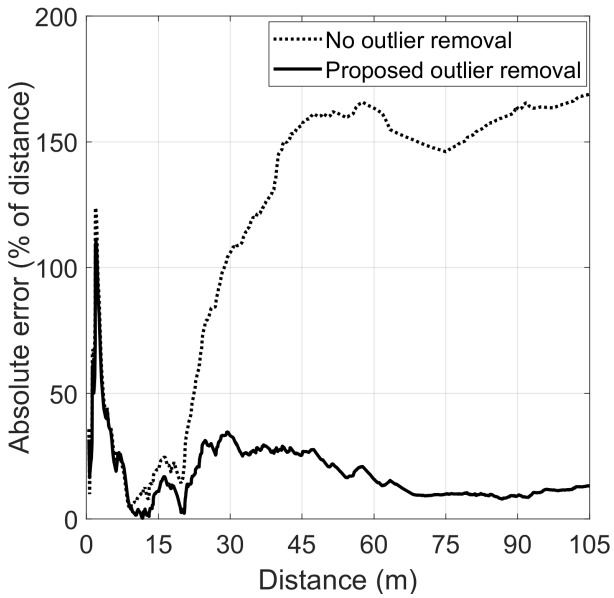

Fig. 19: Example of Radar Odometry with and without outlier removal correction in complex environment. Absolute errors as percentage of covered distance.

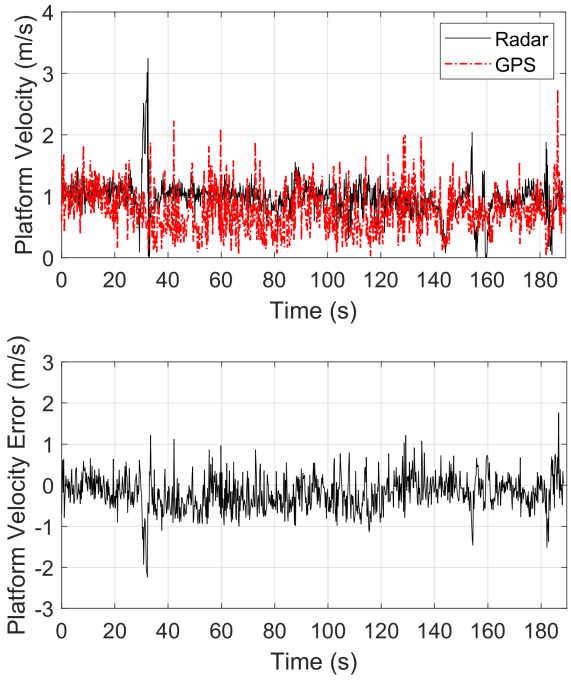

Fig. 20: Comparison between estimated platform velocity and ground truth and Error in platform velocity estimate

to radar odometry results, both as standalone navigation technique as well as when using radar-aided fusion with tightly-coupled Kalman Filter strategy.

Acknowledgment

The author would like to thank Marco Zaccaria Di Fraia for the thorough initial discussion about the topic presented in the paper and Giancarmine Fasano and Alfredo Renga for their support with experimental campaign.

5 References

1 Tiemann, J., Schweikowski, F., Wietfeld, C. 'Design of an uwb indoor-positioning system for uav navigation in gnss-denied environments'. In: 2015 International Conference on Indoor Positioning and Indoor Navigation (IPIN). (, 2007. pp. 613–617

2 Zwirello, L., Xuyang, L., Zwick, T., Ascher, C., Werling, S., Trommer, G.F. 'Sensor data fusion in UWB-supported inertial navigation systems for indoor navigation'. In: IEEE International Conference on Robotics and Automation. (, 2013. pp. 3154–3159

3 Kagawa, T., Li, H.B., Miura, R. 'A UWB navigation system aided by sensor-based autonomous algorithm - Deployment and experiment in shopping mall'. In: International Symposium on Wireless Personal Multimedia Communications, WPMC. (, 2015. pp. 613–617

4 He, K., Zhang, Y., Zhu, Y., Xia, W., Jia, Z., Shen, L. 'A hybrid indoor positioning system based on UWB and inertial navigation'. In: 2015 International Conference on Wireless Communications and Signal Processing, WCSP 2015. vol. 3200. (, 2015. pp. 2–6

5 Li, K., Wang, C., Huang, S., Liang, G., Wu, X., Liao, Y. 'Self-Positioning for UAV indoor navigation based on 3D laser scanner, UWB and INS'. In: 2016 IEEE International Conference on Information and Automation, IEEE ICIA 2016. August. (, 2017. pp. 498–503

6 'Enhanced UAV indoor navigation through SLAM-Augmented UWB Localization'. (IEEE, 2018

7 Tiemann, J., Wietfeld, C. 'Scalable and precise multi-UAV indoor navigation using TDOA-based UWB localization'. In: 2017 International Conference on Indoor Positioning and Indoor Navigation, IPIN 2017. (, 2017. pp. 1–7

8 Kaniewski, P., Kazubek, J., Kraszewski, T. 'Application of UWB modules in indoor navigation system'. In: 2017 IEEE International Conference on Microwaves, Antennas, Communications and Electronic Systems, COMCAS 2017. (, 2018. pp. 1–5

9 Krishnan, S., Sharma, P., Guoping, Z., Woon, O.H. 'A UWB based localization system for indoor robot navigation'. In: 2007 IEEE International Conference on Ultra-Wideband, ICUWB. (, 2007. pp. 77–82

10 Kumar, R., Cousin, J.C., Huyart, B. '2D indoor localization system using FMCW radars and DMTD technique'. In: 2014 International Radar Conference, Radar 2014. (, 2014. pp. 1–5

11 Marck, J.W., Mohamoud, A., Houwen, E., Heijster, R.V. 'Indoor Radar SLAM: A radar application for Vision and GPS Denied Environments'. In: Radar Conference, Proceedings Of the 10th European. (, 2013. pp. 471–474. Available from: https://www.researchgate.net/publication/261092058

12 Vivet, D., Checchin, P., Chapuis, R.: 'Localization and mapping using only a rotating FMCW radar sensor', *Sensors (Switzerland)*, 2013, **13**, (4), pp. 4527–4552

13 Kauffman, K., Raquet, J., Morton, Y., Garmatyuk, D. 'Enhanced feature detection and tracking algorithm for UWB-OFDM SAR navigation'. In: National Aerospace and Electronics Conference, Proceedings of the IEEE. (, 2011. pp. 261–269

14 Deibler, T., Thielecke, J. 'Fusing odometry and sparse uwb radar measurements for indoor slam'. In: 2013 Workshop on Sensor Data Fusion: Trends, Solutions, Applications, SDF 2013. (, 2013.

15 Cole, R., Jameson, B., Garmatyuk, D., Morton, Y.T.J. 'Simultaneous indoor localization and detection with multi-carrier radar'. In: IEEE National Radar Conference. (, 2014. pp. 881–886

16 Baucher, B., Qualls, I., Liang, B., Liu, L., Garmatyuk, D., Morton, Y.T.J., et al. 'Experimental radar-enabled navigation with UWB system in indoor environments'. In: Proceedings International Radar Symposium. (, 2017. pp. 1–8

17 Kauffman, K., Raquet, J., Morton, Y., Garmatyuk, D.: 'Real-time uwb-ofdm radar-based navigation in unknown terrain', *IEEE Transactions on Aerospace and Electronic Systems*, 2013, **49**, (3), pp. 1453–1466

18 Quist, E.B., Beard, R.W.: 'Radar odometry on fixed-wing small unmanned aircraft', *IEEE Transactions on Aerospace and Electronic Systems*, 2016, **52**, (1), pp. 396–410

19 Quist, E.B., Niedfeldt, P.C., Beard, R.W.: 'Radar odometry with recursive-ransac', *IEEE Transactions on Aerospace and Electronic Systems*, 2016, **52**, (4), pp. 1618–1630

20 Scannapieco, A.F., Renga, A., Fasano, G., Moccia, A.: 'Experimental analysis of radar odometry by commercial ultralight radar sensor for miniaturized uas', *Journal of Intelligent and Robotic Systems*, 2018, **90**, (3–4), pp. 485–503

21 Scannapieco, A.F., Renga, A., Fasano, G., Moccia, A. 'Ultralight radar for small and micro-uav navigation'. In: The International Archives of the Photogrammetry, Remote Sensing and Spatial Information Sciences. vol. XLII-2/W6. (ISPRS, 2017. pp. 333–338

22 Mostafa, M., Zahran, S., Moussa, A., El.Sheimy, N., Sesay, A.: 'Radar and visual odometry integrated system aided navigation for UAVS in GNSS denied environment', *Sensors (Switzerland)*, 2018, **18**, (9)

23 IMST. '24 ghz sentire fmcw radar'. (, 2015. [Online; accessed 09-June-2018]. http://www.radar-sensor.com/products/radar-modules/sr-1200/

24 Bosch. 'Bosch medium range radar'. (, . [Online; accessed 21-December-2018]. https://www.bosch-mobility-solutions.com/en/products-and-services/passenger-cars-and-light-commercial-vehicles/driver-assistance-systems/predictive-emergency-braking-system/mid-range-radar-sensor-(mrr)

25 Bosch. 'Bosch long range radar'. (, . [Online; accessed 21-December-2018]. https://www.bosch-engineering.jp/media/jp/pdfs_3/

einsatzgebiete_4/produktdatenblaetter_2/120903_LRR3_EN_V05_final.pdf
26 Folster, F., Rohling, H., Lubbert, U. 'An automotive radar network based on 77 GHz FMCW sensors'. In: IEEE National Radar Conference - Proceedings. (, 2005. pp. 871–876
27 Szullo, A., Seller, R. 'Maneuvering target tracking in wide area multilateration radar system'. In: Proceedings International Radar Symposium. vol. 2016-June. (, 2016. pp. 1–4
28 Sugimoto, S., Tateda, H., Takahashi, H., Okutomi, M. 'Obstacle detection using millimeter-wave radar and its visualization on image sequence'. In: International Conference on Pattern Recognition. vol. 3. (, 2004. pp. 342–345
29 Leys, C., Ley, C., Klein, O., Bernard, P., Licata, L.: 'Detecting outliers: Do not use standard deviation around the mean, use absolute deviation around the median', *Journal of Experimental Social Psychology*, 2013, **49**, (4), pp. 764 – 766. Available from: http://www.sciencedirect.com/science/article/pii/S0022103113000668
30 Rousseeuw, P.J., Croux, C.: 'Alternatives to the median absolute deviation', *Journal of the American Statistical Association*, 1993, **88**, (424), pp. 1273–1283